

*Article*

## Formation of Apatite Coatings on an Artificial Ligament Using a Plasma- and Precursor-Assisted Biomimetic Process

Hiroataka Mutsuzaki<sup>1</sup>, Yoshiro Yokoyama<sup>2</sup>, Atsuo Ito<sup>3</sup> and Ayako Oyane<sup>2,\*</sup>

<sup>1</sup> Department of Orthopaedic Surgery, Ibaraki Prefectural University of Health Sciences, 4669-2 Ami Ami-machi, Inashiki-gun, Ibaraki 300-0394, Japan; E-Mail: mutsuzaki@ipu.ac.jp

<sup>2</sup> Nanosystem Research Institute, National Institute of Advanced Industrial Science and Technology (AIST), Central 4, 1-1-1, Higashi, Tsukuba-shi, Ibaraki 305-8562, Japan; E-Mail: yokoyama.yj@om.asahi-kasei.co.jp

<sup>3</sup> Human Technology Research Institute, National Institute of Advanced Industrial Science and Technology (AIST), Central 6, 1-1-1, Higashi, Tsukuba-shi, Ibaraki 305-8566, Japan; E-Mail: atsuo-ito@aist.go.jp

\* Author to whom correspondence should be addressed; E-Mail: a-oyane@aist.go.jp; Tel.: +81-29-861-4693; Fax: +81-29-861-3005.

*Received: 28 August 2013; in revised form: 8 September 2013 / Accepted: 11 September 2013 /*

*Published: 17 September 2013*

---

**Abstract:** A plasma- and precursor-assisted biomimetic process utilizing plasma and alternate dipping treatments was applied to a Leeds-Keio artificial ligament to produce a thin coating of apatite in a supersaturated calcium phosphate solution. Following plasma surface modification, the specimen was alternately dipped in calcium and phosphate ion solutions three times (alternate dipping treatment) to create a precoating containing amorphous calcium phosphate (ACP) which is an apatite precursor. To grow an apatite layer on the ACP precoating, the ACP-precoated specimen was immersed for 24 h in a simulated body fluid with ion concentrations approximately equal to those in human blood plasma. The plasma surface modification was necessary to create an adequate apatite coating and to improve the coating adhesion depending on the plasma power density. The apatite coating prepared using the optimized conditions formed a thin-film that covered the entire surface of the artificial ligament. The resulting apatite-coated artificial ligament should exhibit improved osseointegration within the bone tunnel and possesses great potential for use in ligament reconstructions.

**Keywords:** plasma surface modification; alternate dipping treatment; apatite; simulated body fluid (SBF); artificial ligament

---

## 1. Introduction

Artificial ligaments are commonly used in ligament operations, including anterior cruciate ligament (ACL) reconstructions, patella tendon repair, and rotator cuff repair, in which the artificial ligaments are inserted in bone tunnels. In particular, the Leeds-Keio artificial ligament (Xiros plc., Leeds, UK), which is composed of poly(ethylene terephthalate) (PET), has been widely used in clinical treatments [1,2]. ACL reconstructions performed using hamstring tendons fixed with staples via Leeds-Keio ligaments in the tibia are called suspensory fixations [1,2]. Because the fixation sites between the soft tissue and the hard tissue are mechanically the weakest regions during the early postoperative period [3,4], the rapid and robust osseointegration of artificial ligaments within bone tunnels is critical for successful ligament reconstruction.

In 2011, Li *et al.* demonstrated that apatite coatings on the surfaces of artificial ligaments are effective in enhancing the osseointegration of artificial ligaments within the bone tunnel [5]. This effect was enabled because apatite is a major inorganic component of natural bone and exhibits good biocompatibility and osteoconductivity [6,7]. In Li's study, an apatite coating was produced on an artificial ligament using plasma surface modification and subsequent immersion in a solution containing apatite powders. The resulting coating comprised micro-sized apatite powders dispersed throughout the ligament surface; however, the majority of the ligament surface remained uncoated. A thin-film apatite coating over the entire surface of a ligament (insertion site) should be beneficial in further enhancing osseointegration within the bone tunnel [8].

Among the various apatite-based thin-film coating techniques, biomimetic processes that employ a simulated body fluid (SBF) [9,10] as the coating solution are especially advantageous in producing bone-like apatite and are even compatible with soft devices composed of low-melting-point polymers [11–13]. Recently, we developed an advanced biomimetic process [13–18] involving a simplified alternating dipping treatment [19]. In this process, a substrate material is precoated with amorphous calcium phosphate (ACP), which is an apatite precursor, using a simplified alternate dipping treatment followed by immersion in SBF [20]. A continuous, thin coating layer of apatite forms on the ACP-precoated substrate within 24 h in SBF. This apatite coating technique, also known as an ACP-assisted biomimetic process [13,21], provides the advantage of simplicity compared with previous biomimetic processes, which require the use of carboxymethylation [22], photografting [23], or sol-gel methods [24,25].

In the present study, we applied the ACP-assisted biomimetic process to a Leeds-Keio artificial ligament to prepare a thin-film apatite coating for improved osseointegration. To optimize the coating conditions, we first prepared hot-pressed plate specimens from Leeds-Keio artificial ligament meshes. The plate specimens were then subjected to plasma surface modification [15–18,26] under various conditions, followed by the alternate dipping treatment and SBF immersion. The quality of the apatite coating on the specimen and the coating adhesion to the specimen surface were evaluated as a function

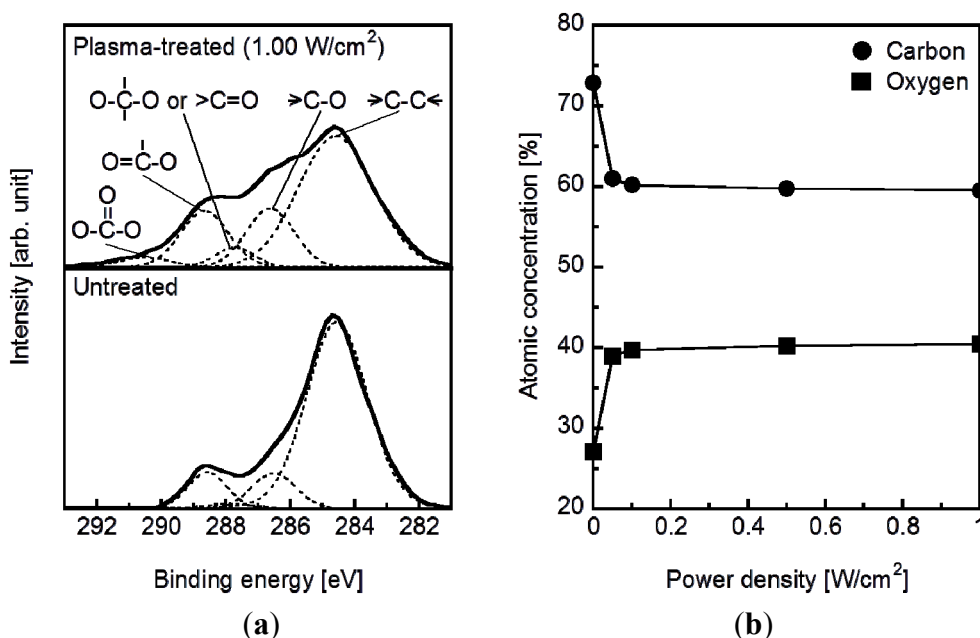
of the conditions (plasma power density) of the plasma surface modification. The resulting optimized coating process was then applied to a Leeds-Keio artificial ligament mesh to demonstrate its potential application in ligament operations.

## 2. Results

### 2.1. Surface Structural Changes due to Plasma Treatment

The plasma surface modification introduced oxygen-containing functional groups to the specimen surface according to the results of X-ray photoelectron spectroscopy (XPS). Figure 1a displays the  $C_{1s}$  XPS spectra of the surfaces of the plasma-treated ( $1.0\text{ W/cm}^2$ ) and untreated plate specimens. The  $C_{1s}$  peaks (solid line) from the plasma treated and untreated specimens were resolved into five peaks (dotted line), which were attributed to the carbon atoms in  $-C-C-$ ,  $-C-O-$ ,  $-C=O/O-C-O-$ ,  $-O-C=O$ , and  $-O-C(=O)-O-$  [27,28]. The peak intensity of the methylene carbon decreased and the intensities of all of the other peaks increased following the plasma treatment. This result can be attributed to the cleavage of the methylene and ester linkages on the specimen surface to produce oxygen-containing functional groups such as hydroxyl, carbonyl, and carboxyl groups. According to the surface composition analysis, the density of the oxygen-containing functional groups on the specimen surface increased after the plasma surface modification with the power densities from  $0.05$  to  $1.00\text{ W/cm}^2$  (Figure 1b).

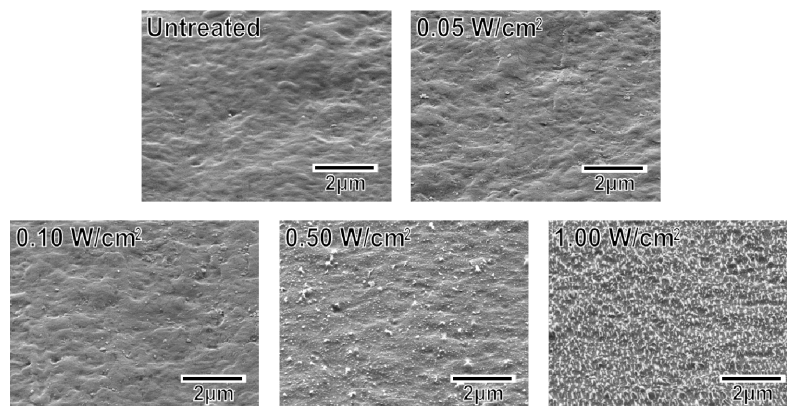
**Figure 1.** (a)  $C_{1s}$  XPS spectra and (b) the surface atomic concentrations of C and O on plasma-treated ( $0.05$ – $1.00\text{ W/cm}^2$ ) and untreated plate specimens.



The surface roughness of the specimens increased with increasing plasma power density. As displayed in the scanning electron microscopy (SEM) images in Figure 2, the untreated specimen and the specimens treated at relatively low plasma power densities ( $0.05$  and  $0.10\text{ W/cm}^2$ ) exhibited smooth surfaces. The specimens treated at higher plasma power densities ( $0.50$  and  $1.00\text{ W/cm}^2$ ) exhibited surfaces with submicron-sized granules. In addition, the granules on the specimen surface increased in

number density with increasing plasma power density. These granules most likely formed via the cleavage of the methylene and ester linkages at the specimen surface and the subsequent etching of the degraded portion during the plasma treatment [29].

**Figure 2.** SEM images of the surfaces of the untreated and plasma-treated ( $0.05\text{--}1.00\text{ W/cm}^2$ ) plate specimens.



## 2.2. Surface Structural Changes due to the Alternate Dipping Treatment

Following the alternate dipping treatment, an ACP precoating formed on the plasma-treated plate specimens (P005, P010, P050, and P100) but not on the untreated plate specimen (P000). According to the XPS results, calcium phosphate was deposited on the surfaces of all of the plate specimens except for P000 (Figure 3). According to our previous transmission electron microscopy results, the calcium phosphate was most likely in the form of ACP [20]. The ACP precoating slightly altered the morphology of the specimen surfaces, as revealed in the SEM images in Figure 4. The ACP precoatings were apparently uniform and covered the entire surfaces of the specimens.

**Figure 3.** XPS spectra of the surfaces of the plate specimens P000, P005, P010, P050, and P100.

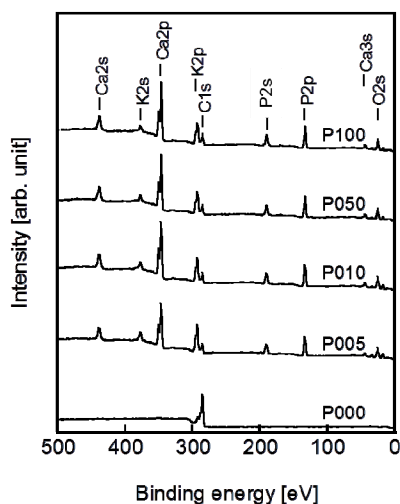
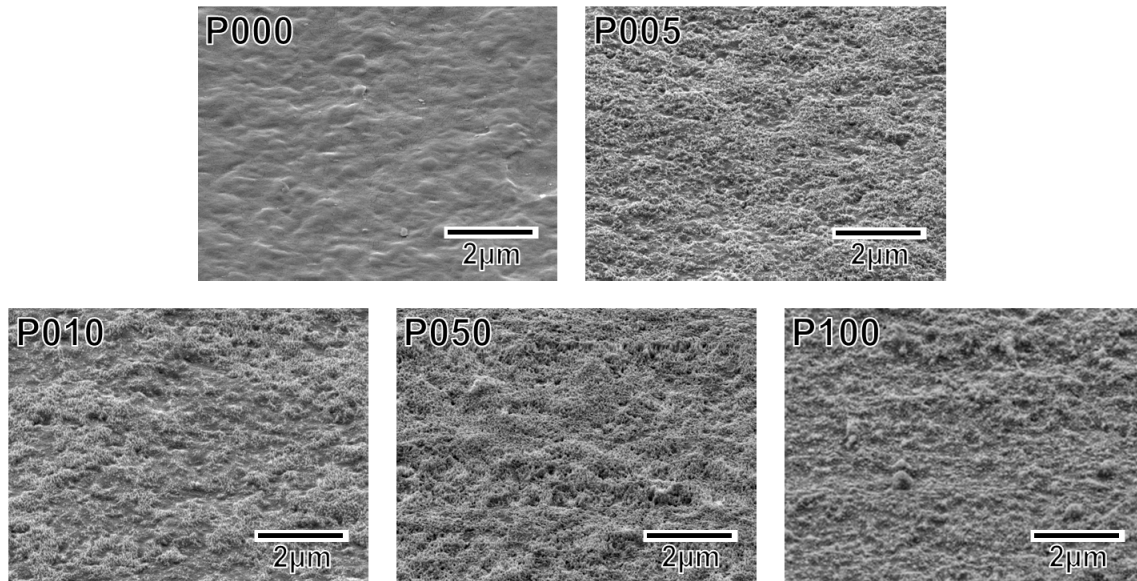




**Figure 4.** SEM images of the surfaces of the plate specimens P000, P005, P010, P050, and P100.



### 2.3. Surface Structural Changes due to SBF Immersion

A thin coating of apatite formed on the ACP-precoated plate specimens (P005, P010, P050, and P100) following a 24 h immersion in SBF (Figure 5). The apatite coating exhibited a nano-porous structure and covered the entire surfaces of the specimens. According to the results of thin-film X-ray diffractometry (TF-XRD), this coating layer was composed of low-crystalline apatite [30] (Figure 6). On the P000 plate specimen without the ACP pre-coating, no coating layer was observed following the immersion in SBF (Figures 5 and 6). These results correspond well with our previous results from other polymer substrates [15–18,26].

**Figure 5.** SEM images of the surfaces of the plate specimens P000, P005, P010, P050, and P100 following immersion in SBF for 24 h.

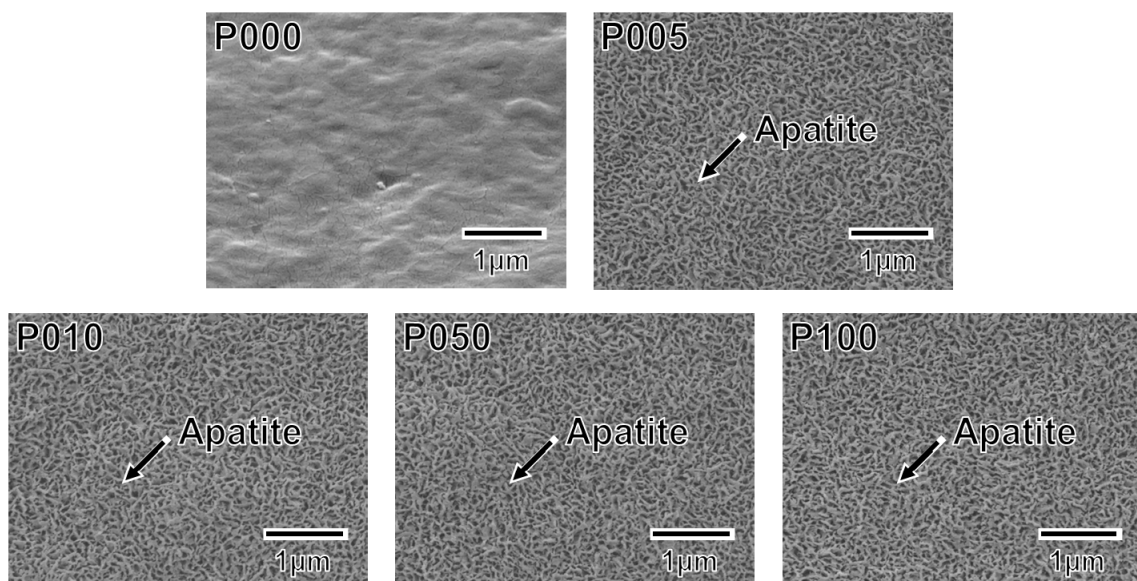
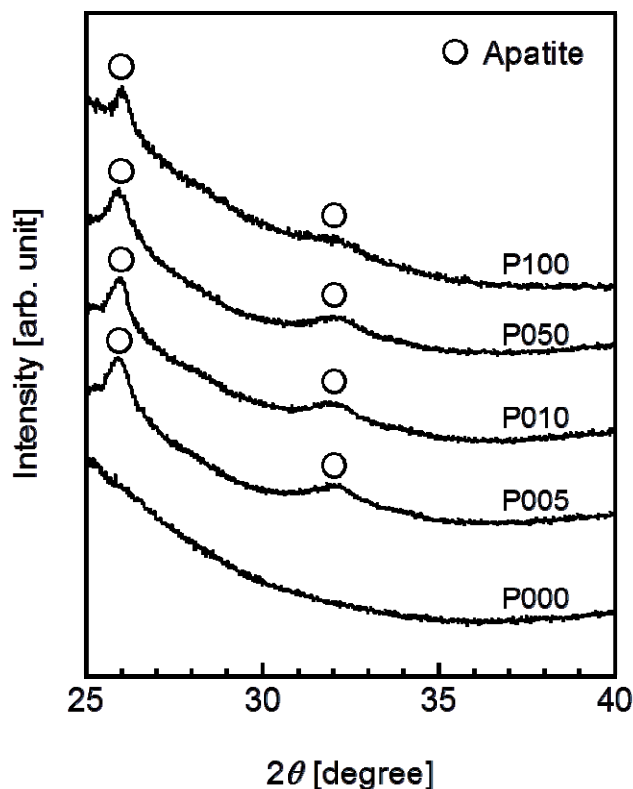


**Figure 6.** TF-XRD patterns from the surfaces of the plate specimens P000, P005, P010, P050, and P100 following immersion in SBF for 24 h.



#### 2.4. Adhesion Strength of the Apatite Coating to the Specimen

The adhesion strength of the apatite coating to the plate specimen improved with the use of increasing plasma power density for the plasma surface modification. P005 was excluded from the adhesion strength measurement based on the results of a screening test in which the coating layer detached from the specimen surface using a Scotch<sup>®</sup> tape-detachment test. The apatite coatings on the plate specimens treated with higher plasma powers (P010, P050, and P100) remained adhered even after the tape-detachment test and were therefore subjected to the quantitative adhesion strength measurement. It can be observed in Figure 7 that the adhesion strengths of the apatite coatings to the P050 and P100 surfaces were significantly higher than that to the P010 surface ( $p = 0.0015$  and  $p < 0.0001$ , respectively). The average adhesion strength of the apatite coating to the P100 surface was higher than that to the P050 surface, although the difference was not statistically significant. According to the energy dispersive electron probe X-ray analysis (EDX) of the fractured surfaces, the fracture occurred at the coating-specimen interface for P010 and P050. For these specimens, Ca and P, which are component elements of apatite, were detected by EDX on the jig side, whereas they were not detected on the specimen side (Figure 8). The fracture in P100 occurred not only at the coating-specimen interface but also at the coating-glue interface. In the case of P100, a splintered layer composed of Ca and P was observed on both the jig and the specimen sides (Figure 8).

**Figure 7.** Adhesion strengths of the apatite coatings to the surfaces of the plate specimens P010, P050, and P100 ( $n = 7$ ,  $* p < 0.05$ ).

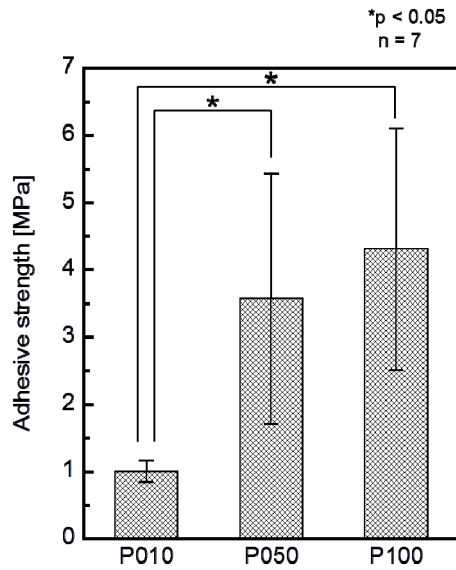


**Figure 8.** SEM (upper left image in a set of 4 images) and EDX (C, Ca, P) images of the specimen side and jig side fractured surfaces, after the measurement of adhesion strength of the apatite coatings to the surfaces of the plate specimens P010, P050, and P100.

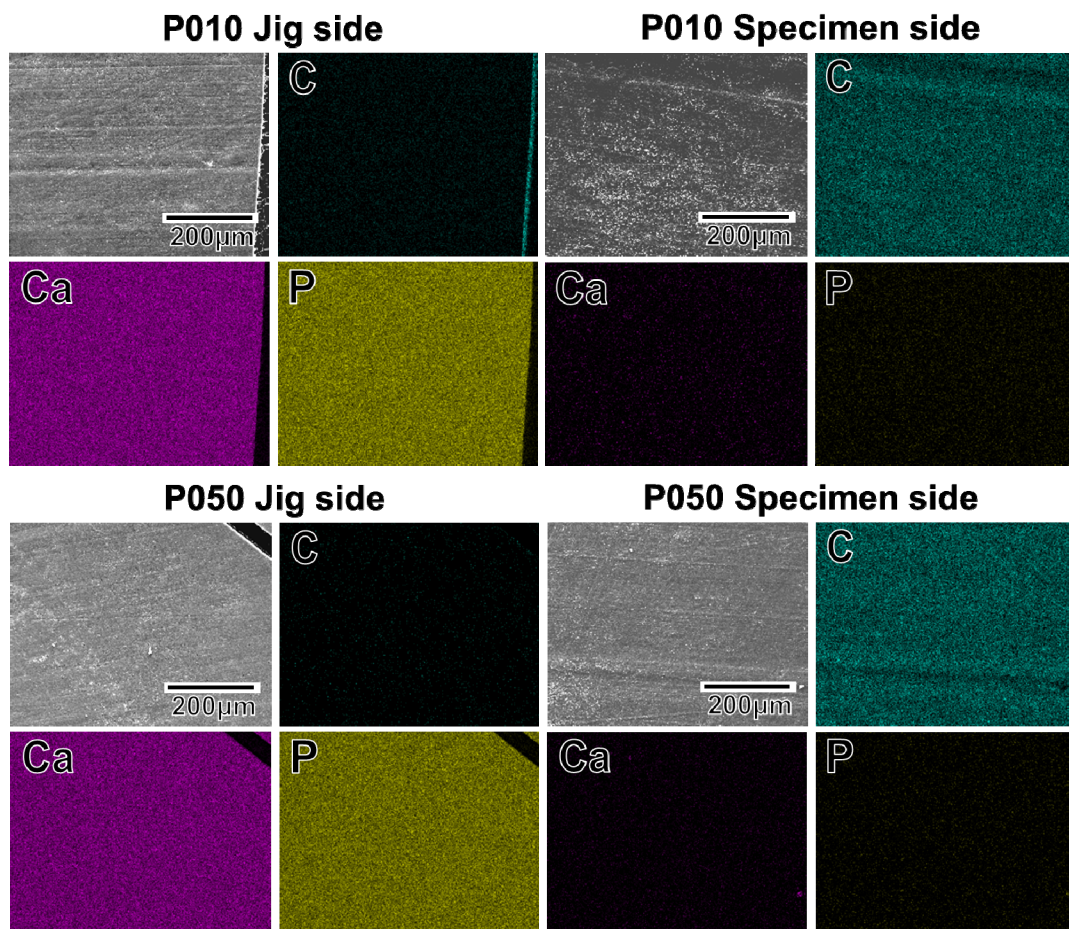
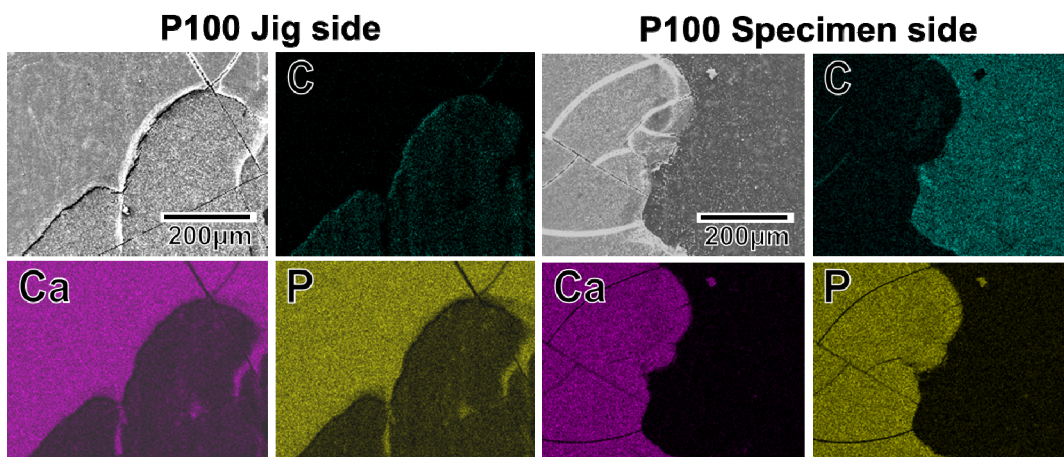




Figure 8. Cont.



### 2.5. Application to Artificial Ligament Meshes

An apatite coating layer was successfully deposited on the mesh specimen as well as on the plate specimens. Figure 9 displays SEM images of the surfaces of (a) the untreated (as-prepared) mesh specimen and (b) the P100 plasma-treated mesh specimen following a 24 h immersion in SBF. As displayed in Figure 9b, the individual fibers composing the artificial ligament were fully coated with a continuous thin-film apatite layer exhibiting a nano-porous structure similar to that formed on the plate specimens (see P100 in Figure 5).

Figure 9. SEM images collected at varying magnifications from (a) the untreated mesh specimen and (b) the P100 mesh specimen after a 24 h immersion in SBF.

